ASSESSING SUSCEPTIBILITY TO CHROMIUM CARBIDE PRECIPITATION IN Cr-Mn AUSTENITIC STAINLESS STEEL WELDS

Amuda, M.O.H.*[1], Enumah, K.S[2], Onitiri, M.A.[3] and Osoba, L.O.[4]
[1, 2, 4] Materials Development and Processing Research Group, Department of Metallurgical and Materials Engineering, University of Lagos, 101017
[3] Department of Mechanical Engineering, University of Lagos, Nigeria, 101017
*Corresponding author: amuda@unilag.edu.ng

ABSTRACT
Chromium-manganese austenitic stainless steel is a low cost grade with metallurgical and mechanical properties approximating a standard nickel-chromium austenitic stainless steel. It serves as a good substitute to the standard nickel-chromium grade owing to the high cost of nickel. But, there is little information on its weldability particularly the influence of welding parameters on chromium carbide precipitation in the heat affected zone. This limits its structural application through fusion welding. Therefore, in this paper, carbide precipitation in chromium-manganese austenitic stainless steel welds was investigated in the heat input range 180 - 300 J/mm under different combinations of arc current and welding speeds. Microstructural analysis after 10% oxalic acid electrolytic etch revealed that increasing heat input produced significant changes in microstructure of the welds with wider sensitized structure at heat input greater than 206 J/mm. Microstructure of welds produced at heat input lower than 206 J/mm was free of chromium carbide precipitation. This level of heat input which corresponds to arc current of 110 -125A and welding speeds in the range 319- 395 mm/min show that sensitized region associated with chromium carbide precipitation can be safely avoided during fusion welding of this grade of austenitic stainless steel through carefully selected welding parameters.

Keywords: Austenitic Stainless Steel Weld, Chromium Carbide Precipitation, Heat Affected Zone, Microstructure, Welding Parameters

INTRODUCTION
Among the stainless steel group, the austenitic variety is the workhorse of the group representing about 75% of the market share with the ferritic, martensitic, duplex and precipitation hardening varieties taking up the balance (www.worldstainlessteel.net, 2016; Charles *et al*., 2009). This more than three-quarter dominance is due to the wide range of service compliant properties in the grade; which are not readily obtainable from other varieties. Ordinarily, stainless steels are iron-carbon-chromium based materials differentiated into the various

grades by the concentration of other alloying elements most significantly, nickel, in stabilizing the various phases such as austenite, ferrite, martensite, duplex and precipitation hardening phases.

The austenitic variety is usually chromium-nickel alloy with face centred cubic (FCC) crystal structure containing more than 12wt. % chromium. The FCC crystal structure confers on the austenitic grade excellent ductility and formability; and thus, it exhibits superior mechanical properties relative to the other varieties (Lo *et al*., 2009). Consequently, the grade is extensively used in the chemical and petrochemical, oil and gas, food processing, defense and armoury, construction and transportation industries where corrosion and/or high temperature oxidation are major concerns (Baek *et al*., 2001). But recently, the comparatively higher price of nickel with respect to other alloying elements has pushed up the cost of the standard austenitic grade. This has generated the incentive for the production of an alloy with approximate properties to the standard 300 Series (18Cr-8Ni) austenitic grade but with cheaper elements substituting for the nickel (McGuire, 2008). Nickel being both an austenite former and stabilizer ensures that the 18Cr-8Ni stainless steel is austenitic at both elevated and room temperatures while also contributing to the corrosion resistance of the steel. It equally lowers the martensite transformation temperature, which assists in preventing the formation of brittle martensitic structure (Coetzee and Pistorious, 1996). Thus, any element substituting nickel must offer these excellent characteristics at competitive cost.

A wide range of economical low nickel austenitic stainless steels combining low cost with good formability and properties similar to those of standard grades are now available accounting for about 10% of the total stainless steel market. These grades include the Cr-Mn-N and Cr-Mn-Cu stainless steel varieties (International Stainless Steel Forum (ISSF), 2005). The Cr-Mn-Cu variety is a new entrant with different chemistries characterised by reduced chromium at about 15% and extra low nickel content. Furthermore, nitrogen is replaced with copper to improve working property but this grade possesses low mechanical properties and its corrosion resistance is just adequate particularly in mildly corrosive environments (ISSF, 2005). Copper is considered a minor alloying element in this new grade austenitic stainless steel with a concentration of between 1 – 4 %. Because of the cap on the concentration of copper in this sub-grade austenitic stainless steel, it is usually not indicated in the nominal composition of the alloy. The alloy is therefore simply represented as Cr-Mn austenitic stainless steel grade.

This new sub-grade austenitic stainless steel is more affordable and as such finds application in several industries including architectural/building construction, food and beverages, transportation, chemical, electrical machinery/equipment, water supply and household consumables. In many of these applications, fusion welding is an integral manufacturing route for fabricating complex structures and components, and also in corrective maintenance. However, the process is known to have significant effects on the microstructure of the resolidified metal and thus, is expected to have strong influence on the corrosion and mechanical properties of the welded samples (Urade and Ambade, 2016).

There are many problems associated with the fusion welding of stainless steel. These include sensitization of the heat affected zone (HAZ) particularly in the high temperature region which is adjacent to the fusion zone interface, hot cracking of weld metal and impaired corrosion resistance. Mechanism of sensitization involves the formation of chromium depleted zone adjacent to the grain boundaries during high temperature processes such as obtainable in welding. Incidentally for the standard austenitic grade, extensive pool of knowledge and experience has been built-up on its weldability from myriads of studies and field feedbacks in several application environments. But the new Cr-Mn-Cu variety has such no privilege of body of knowledge and experience. This implies that the increase in the production and use of the new Cr-Mn-Cu grade is not currently matched by an adequate level of user knowledge; particularly, the influence of fusion heat on the sensitization of the welded grade (ISSF, 2005). Thus, there is a risk that the grade may be inappropriately specified for service in the welded condition. Further, lack of understanding of the influence of in-service conditions on creating a predisposing factor for the onset of sensitization in the material is equally a challenge.

Therefore, it is the focus of the present investigation to provide an understanding for the influence of welding process parameters on sensitization behaviour in a new Cr-Mn austenitic stainless steel weld. Sensitization behaviour in this instance is evaluated in terms of the precipitation of chromium carbide in the HAZ of the welds. The process parameters considered in this are the arc current and the electrode traverse speed. This work represents an indigenous effort at examining the weldability of the new Cr-Mn austenitic stainless steel within the Nigerian context.

MATERIALS AND METHODS

The stainless steel material for the investigation, received in the form of 3 mm thick sheet, was sectioned into coupons of dimension 150 mm x 75 mm and then subsequently grit blasted to clean the surface followed by deep agitation in a solution of benzene for 5 minutes to remove adhering dirt and grease. The chemical composition of the steel presented in Table 1 was determined using ThermoFisher Scientific's High End Optical Emission Spectrometer. Autogenous full bead on plate weld was produced using direct current straight polarity (DCEN) arc torch from a Tungsten Inert Gas (TIG) machine at constant voltage of 20V. The range of arc current and electrode traverse speed established for TIG torch melting of thin gauge AISI 430 ferritic stainless steel welds by Amuda (2011) and Amuda and Mridha (2009) was adapted for the present work. This is because thermal cycle dynamics in welded piece is influenced more by the thickness rather than the materials composition (Easterling, 1992). Thus, the combination of the process parameter used for the welding is provided in Table 2. The fusion heat delivered to the coupons was calculated from Eq. (1), where Q is the heat input (J/mm), V is the potential difference across the terminals (V), I is the arc current (A), ν is the electrode traverse speed (mm/min.) and η is the efficiency of the TIG welding process (0.48) (Amuda and Mridha, 2011). Seven welded pieces were produced from the combination of process parameters listed in Table 2. The welded specimens were observed for physical defects such as melt-through (craters) and deformation (distortion) before further characterisation.

$$Q(J/mm) = \frac{V \bullet I}{\upsilon} \times \eta \qquad (1)$$

Table 1: Chemical composition of stainless steel sheet

Materials	***Elemental Composition (wt. %)***									
	Fe	C	Si	Mn	P	S	Cr	Ni	Cu	Trace Element
Austenitic Stainless Steel Sheet	72.70	0.07	0.45	10.15	0.05	0.01	14.89	0.34	1.12	Bal.

Table 2: Matrix of process parameter combinations

Weld Coupons	Current (A)	Welding Speed (mm/min)	Voltage (V)	Heat Input (J/mm)
WC 1	50	95	20	302
WC 2	70	171	20	235
WC 3	90	177	20	293
WC 4	110	319	20	198
WC 5	117	349	20	193
WC 6	125	395	20	182
WC 7	150	417	20	207

The welded coupons were sectioned transverse to the welding direction and prepared for metallographic procedures using standard technique available in the literature (Vander Voort, 1999). The microstructure of the un-welded base metal was characterized by immersion etching in a solution of aqua regia (100 ml HCl + 33 ml HNO_3 + 100 ml C_2H_5OH) before sensitization test. Chromium carbide precipitation, evaluated in terms of sensitization of the welds, was investigated via 10% oxalic acid electrolytic etch using an *in-house* developed kit conforming to the standard provided in ASTM A 262 (2004). The circuit diagram for the *in-house* purpose-built rectifier is presented in Fig.1 together with the set-up for the oxalic acid etch.

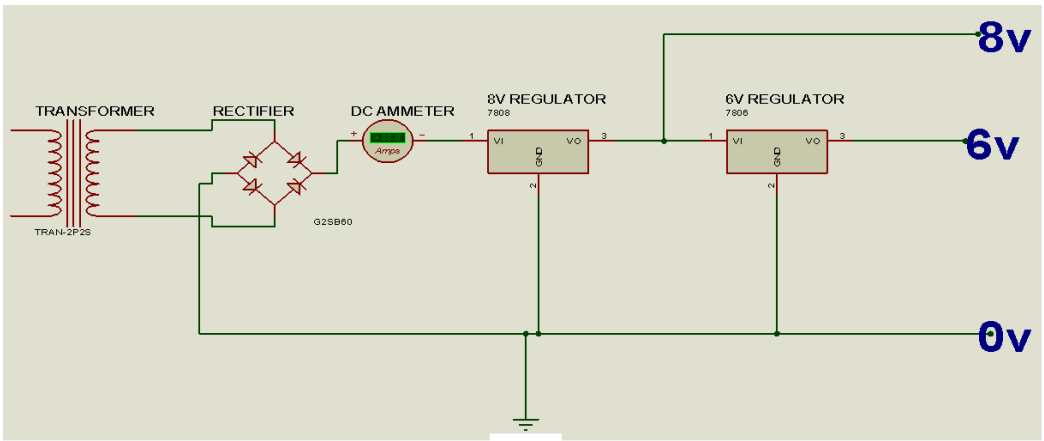

(a)

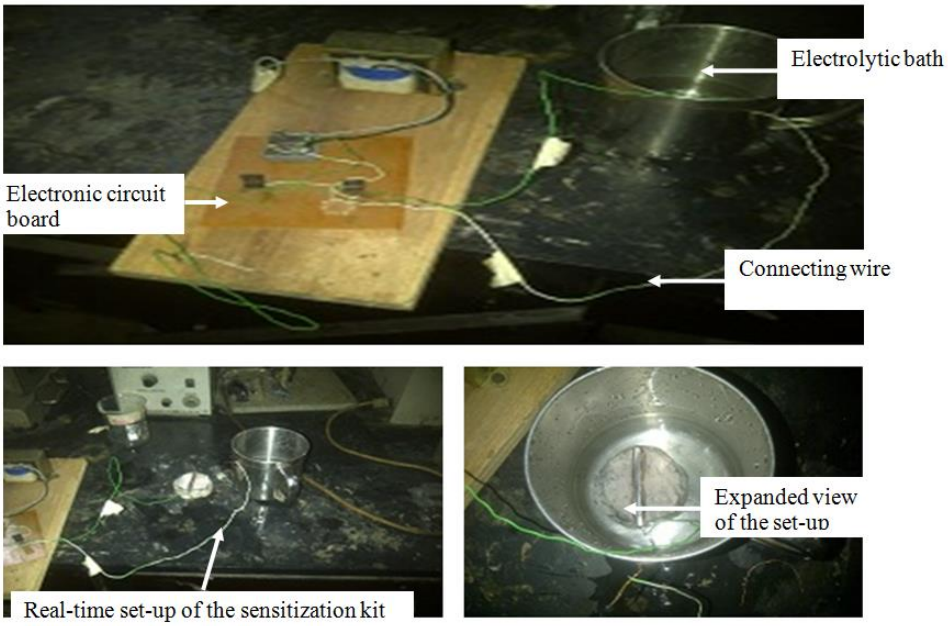

Fig.1: ***In-house*** **purpose built sensitization kit: (a) circuit diagram and (b) sensitization set up**

RESULTS AND DISCUSSION

Composition and Microstructure of Base Metal

The result of spectrochemical analysis presented in Table 1 listed the major elements in the base metal as Cr, Mn and Cu at 14.89%, 10.15% and 1.12%, respectively with Ni at 0.34%. This range of composition corresponds to the new series of austenitic stainless steel with extra low nickel in which nitrogen has been replaced with Cu and Ni substituted by Mn to reduce cost and improve workability (ISSF, 2005). These new series of affordable Cr-Mn-Cu austenitic stainless are generically referred to as the 200 grades. The microstructure of the base metal shown in Fig. 2 revealed an equiaxed fully austenitic matrix with some dispersed carbides inter and intra-granularly within the austenite grains. The figure confirms that the base metal is indeed an austenitic stainless steel material. Sudhakaran *et al*., (2014) reported similar microstructural morphology in the base metal of un-welded AISI 202 austenitic stainless steel.

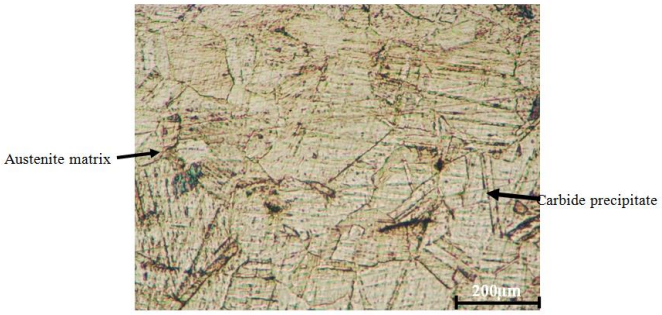

Fig. 2: Microstructure of un-welded austenitic stainless steel base metal

Topography and Microstructure of Resolidified Welds

The topography of some of the welded coupon shown in Fig. 3 revealed a smooth continuous weld track without any physical defects such as melt-through or cracks. This indicates that adoption of the range of process parameters used by Amuda and Mridha (2009) for thin gauge ferritic stainless steel welds for the welding of Cr-Mn-Cu austenitic stainless steel was appropriate.

Fig. 3: Topography of some of the welded coupons

The microstructure of the resolidified weld track is influenced by the solidification mode of the austenitic stainless steel welds; and this is mainly determined by the chemical composition, and in particular, by the balance of austenite and ferrite-forming elements. Literature indicates that welding parameters only have secondary influence on the microstructure of the resolidified weld (Lippold and Kotecki, 2005). Equivalent diagrams such as the Welding Research Council (WRC) and Schaeffler diagrams are used in predicting the solidification microstructure of welds by establishing the relationship between austenite- and ferrite-forming elements in the form of Ni (Ni_{eq}) and Cr-equivalent (Cr_{eq}) diagrams (Fig.4). The Ni and Cr-equivalent relationship (Eq. (2) and Eq.

(3)) adapted from Lippold and Kotecki (2005) and Speidel (2006) in relation to the spectra-compositions listed in Table 1 demonstrates that the ratio of Ni_{eq}/Cr_{eq} is 7.73/15.63. Schaeffler diagram (Fig. 4b) predicts that austenitic stainless steel with this Ni_{eq}/Cr_{eq} ratio will solidify with a primary structure of δ-ferrite as leading phase (the Ferrite and FA fields on the diagram) and retain varying amounts of high temperature δ-ferrite in the ambient temperature microstructure of the weld. Fig. 5 is the room temperature microstructure of the resolidified weld coupons consisting of austenite matrix with sparse distribution of vermicular (feathery) δ-ferrite. du Toit (1999) reported similar primary solidification structure in chromanite^{TM} austenitic stainless steel welds.

Sensitization Characterization in Oxalic Acid Etched Weld Samples

Sensitization represents the means of evaluating the susceptibility of stainless steels to chromium carbide precipitation which facilitates intergranular corrosion. ASTM A 262 (2004) provides acceptance criteria for oxalic acid etch test depending on the state of the grain boundary. The detail of the classification is presented in Table 3 and these criteria are used to screen the microstructures of the HAZ of the weld section for susceptibility to sensitization.

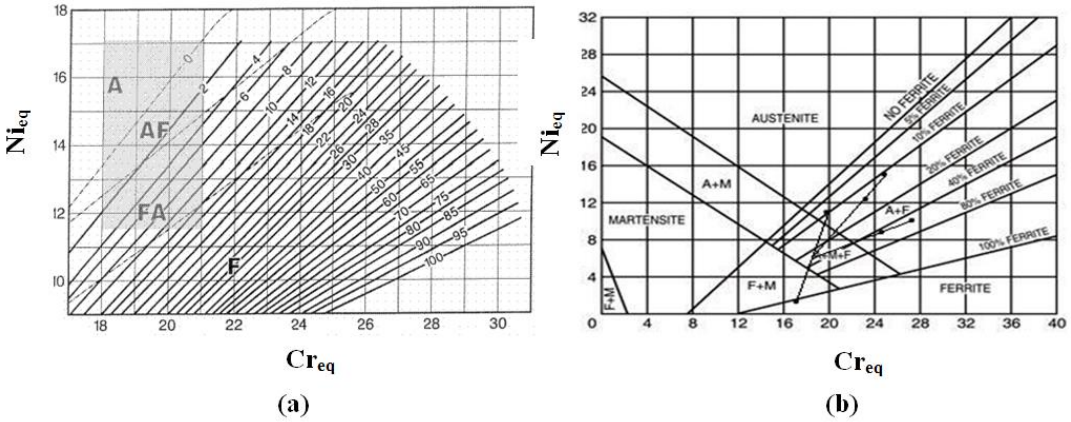

Fig. 4: Equivalent diagrams for predicting solidification microstructures of stainless steel welds: (a) WRC 1992 diagram and (b) Schaeffler diagram (Lippold and Kotecki, 2005)

$$Ni_{eq} = Ni + 30C + 0.1Mn - 0.001(Mn)^2 + 18N + 0.33Cu \quad (2)$$

$$Cr_{eq} = Cr + 1.5Si + Mo + 0.7Nb \quad (3)$$

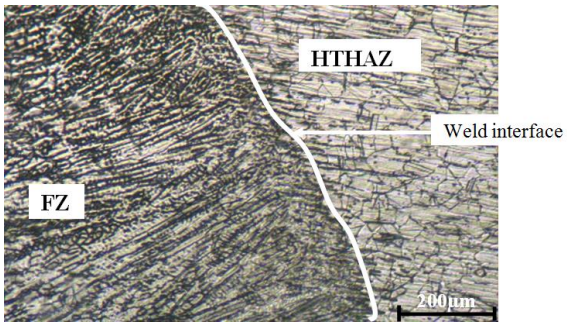

Fig.5: Microstructure of resolidified weld metal showing fully austenitic matrix and vermiculite ferrite elongated in the direction of solidification with the various regions around the weld

Table 3 Classification of microstructure in 10% oxalic acid electrolytic etch (ASTM 262, 2004)

Classification	State of the microstructure
Acceptable	1.Step structure: step only between grains, no ditches at the grain boundary. 2.Dual structure: some ditches at the grain boundary in addition to steps, however, no single grain is completely surrounded by ditches.
Unacceptable	Ditch structure: one or more grains is/are completely surrounded by ditches.

Fig.6 shows the microstructure of the HTHAZ region of the welded samples produced at different heat inputs after 10% oxalic acid electrolytic etching. The figure demonstrates that the response of the microstructure to oxalic acid etch is influenced by heat input. The microstructures of welds produced at heat input in the range 182-198 J/mm (Figs.6a-c) are essentially free of any grain boundary phenomenon such as the presence of ditched structure or step grains or a network of ditches. But those produced at heat input in the range 207-302 J/mm exhibit either the presence of step grains, ditches or network of ditches (Figs. 6d-g).

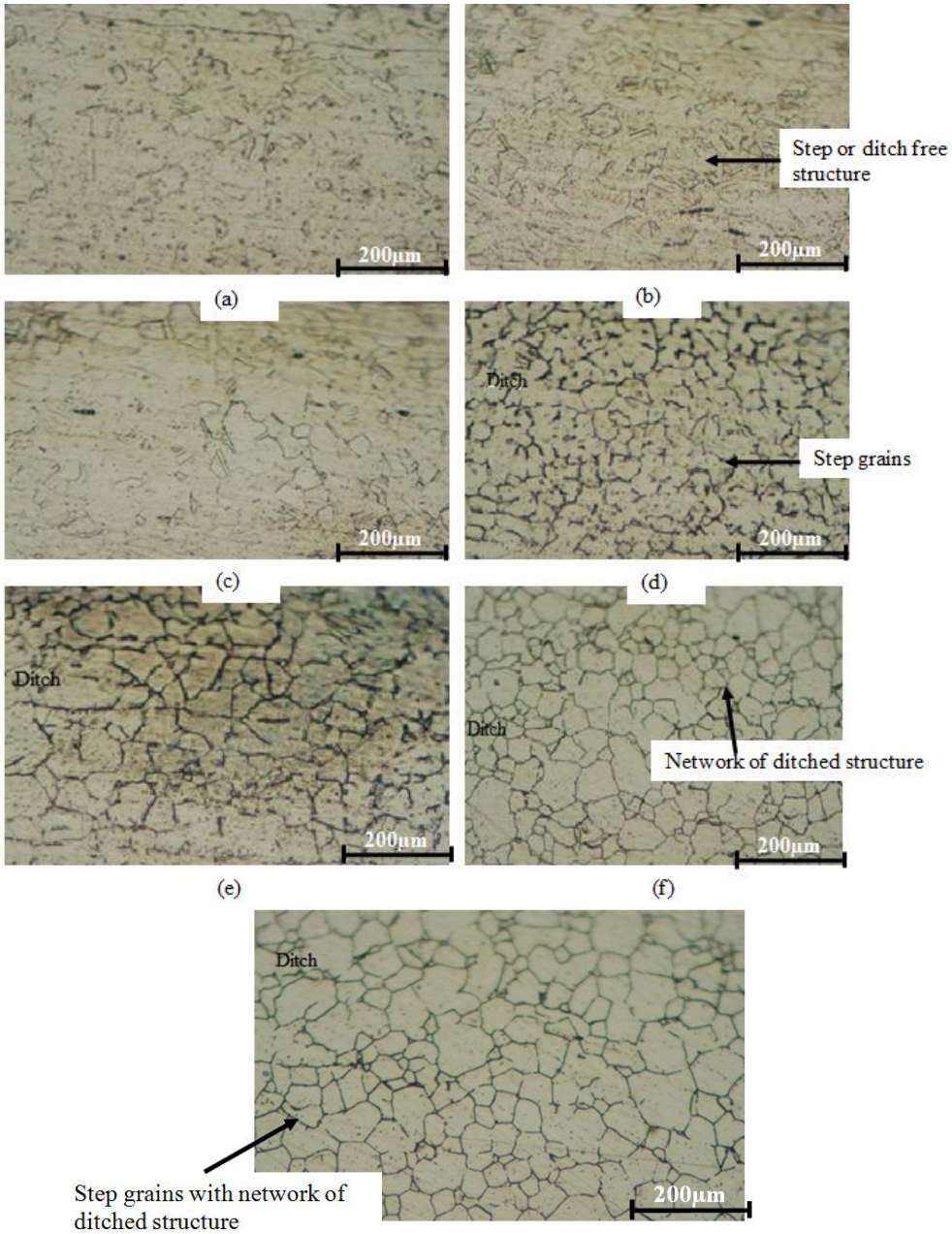

Fig.6: Influence of heat input on response of weld to sensitization: (a) 182, (b) 193, (c) 198, (d) 207, (e) 235, (f) 293 and (g) 302 J/mm

Two streams of behaviour are apparent in this analysis in relation to the criteria listed in Table 3. Weld tracks produced with heat input less than 200 J/mm

exhibit acceptable response to 10% oxalic acid etch while those produced with heat input greater than 206 J/mm are susceptible to sensitization. Thus, it appears that there is a relationship between heat input and susceptibility to sensitization in this new Cr-Mn-Cu austenitic stainless steel. Therefore, benchmarking the state of the microstructures in Fig.6 with the criteria listed in Table 3 indicates that the welds produced with heat input less than 200 J/mm generally pass the sensitization test though the degree of ditching increases as the heat input increases. Therefore, these welds are not likely to experience intergranular corrosion in service when fabricated with the range of heat input within this domain. Literature reports that confirmation of sensitized zones in the HTHAZ is an indication of carbide precipitation particularly chromium carbide. But this must be confirmed with an SEM/EDX analysis (Lippold and Kotecki, 2005). The characteristics observed in the microstructures in this study are consistent with those seen in the corresponding HTHAZ region of 304 austenitic stainless steel welds by Kumar *et al*., (2015). They reported that the development of sensitized regions was observed to increase in welds produced with higher heat inputs and decreased in those produced with lower heat inputs.

Moreover, literature indicates that heat input is an important parameter affecting the susceptibility to intergranular corrosion resistance in welds since it can induce segregation of alloying elements and formation of chromium-depleted zones (Dadfar *et al*., 2007). Furthermore, the same parameter controls the cooling rate within the HTHAZ which determines the residence time spent within the transformation range.

The cooling rates of the various welds estimated using Rosenthal analytical relationship (Poorhaydari *et al*., 2005) for thin gauge materials is shown in Fig. 7. The figure reveal that the cooling rates for welds produced by heat input in the range 182-198 J/mm is 20^{o}C/s-16.4^{o}C/s while those with heat input in the range 207-302 J/mm is 14.3^{o}C/s-4.8^{o}C/s. These ranges of cooling rates indicate that rapid cooling associated with low heat input suppresses carbide precipitation. This is accomplished by ensuring that the carbon, which drives precipitation, is kept in solution. On the other hand, high heat input corresponding to slow cooling rate results in longer residence time in the sensitization temperature range. This increases the propensity to chromium carbide precipitation in welds (Kumar and Reddy, 2013). van Warmelo (2006) similarly reported that a reduction in heat input increases cooling rate in austenitic stainless steel welds resulting in lower incidence of chromium carbide precipitation. Osoba *et al*., (2013) equally reported that at low heat input, steep thermal gradient is generated, while at high

heat input shallow thermal gradient occurs. By implication, the shallow thermal gradient allows considerable time for chromium depletion along grain boundaries which is not permissible in steep thermal gradient associated with low heat input welds. The range of heat input producing sensitization free welds corresponds to arc current of 110 -125A and welding speeds in the range 319- 395 mm/min. The welds produced with this range of process parameters are equally defect free (Fig. 6a-c).

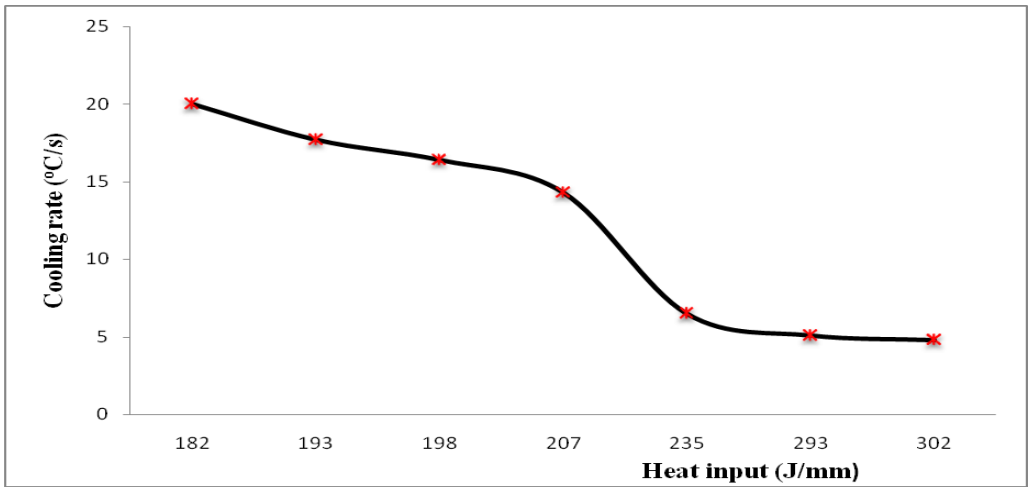

Fig. 7: Influence of heat input on cooling rate in the HTHAZ of Cr-Mn-Cu austenitic stainless steel welds

CONCLUSION

Susceptibility of the weld of a new Cr-Mn austenitic stainless steel grade to chromium carbide precipitation via sensitization analysis has been undertaken. Microstructural analysis indicates that heat input has a strong influence on sensitization behaviour in the welds. In specifics, microstructure of welds produced at heat input lower than 206 J/mm was free of sensitization because of the very low chances of chromium carbide precipitation. But, those produced at heat input in the range 207-302 J/mm exhibit strongly sensitized structures. This was attributed to the time spent within the transformation range. Welds produced with heat input less than 206 J/mm have a cooling rate in the range 20^{o}C/s-16.4^{o}C/s which ensures that carbon is locked in solution unlike those produced with higher threshold of heat input with cooling rate in the range 14.3^{o}C/s-4.8^{o}C/s. The range of heat input for avoiding sensitization in Cr-Mn austenitic stainless steel welds established in this study corresponds to arc current 110 -

125A and welding speeds 319- 395 mm/min. This range of welding process parameters equally produces defect free welds.

ACKNOWLEDGMENT

The technical staff of the Central Workshop, Faculty of Engineering, University of Lagos, Nigeria are appreciated for providing technical assistance for the welding of the coupons. Engineer Hisham Muhammed of the Department of Electrical/Electronic and Computer Engineering of the same institution is equally acknowledged for his input in the development of the circuit diagram.

REFERENCES

Amuda, M.O.H. (2011). Microstructural features and properties of TIG melted AISI 430 ferritic stainless steel welds, Ph.D. Thesis, International Islamic University Malaysia.

Amuda, M.O.H. and Mridha, S. (2009). Microstructural features of AISI 430 ferritic stainless steel (FSS) weld produced under varying process parameters. *Int. J. Mech. Mater. Eng*., **4(2)**:160-166.

Amuda, M.O.H. and Mridha, S. (2011). Effect of energy input on microstructure and hardness of TIG welded AISI 430-ferritic stainless steel. *Adv. Mater. Res*., **264**: 390-396.

ASTM A 262 (2004). Standard practices for detecting susceptibility to intergranular attack in austenitic stainless steels. ASTM International, Pennsylvania.

Baek, J.H., Kim, Y.P., Kim, W.S. and Kho, Y.T. (2001). Fracture toughness and fatigue crack growth properties of the base metal and weld metal of a type 304 stainless steel pipeline for LNG transmission. *Int. J. Press. Vessels Pip*., **78(5)**:351-357.

Charles, J., Mithieux, J.D., Santacreu, P.O. and Peguet, L. (2009). The ferritic stainless family: the appropriate answer to nickel volatility?. *Revue de Métall.*, **106(3)**:124-139.

Coetzee, M. and Pistorious, P.G.H. (1996). The welding of experimental low-nickel Cr-Mn-N stainless steels containing copper. *J. South African Inst. Min. Metall*., **96 (3)**:99-108.

Dadfar, M., Fathi, M.H., Karimzadeh, F., Dadfar, M.R. and Saatchi, A. (2007). Effect of TIG welding on corrosion behavior of 316L stainless steel. *Mater. Lett*., **61 (11)**:2343-2346.

du Toit, M. (1999). The microstructure and mechanical properties of Cromanite™ welds. *J. South African Inst. Min. Metall*., **99 (6):**333-39.

Easterling, K. (1992). Introduction to the Physical Metallurgy of Welding, Second Edition. Butterworth-Heinemann Ltd. Oxford

ISSF (2005), New 200-Series Steels: An Opportunity or a Threat to the Image of Stainless Steel, pp. 1-11. ISSF, Brussels.

Lippold, J.C. and Kotecki, D.J. (2005). Welding metallurgy and weldability of stainless steels, second edition, Wiley & Sons Inc., Hoboken.

Kumar, M. V., Balasubramanian, V., Rajakumar, S. and Albert, S. K. (2015). Stress corrosion cracking behaviour of gas tungsten arc welded super austenitic stainless steel joints. *Def. Technol*., **11(3)**: 282-291.

Kumar, D.H. and Reddy, A.S. (2013). Study of mechanical behavior in austenitic stainless steel 316LN welded joints. *Int. J. Mech. Eng. Rob. Res*., **2(1)**:37-56.

Lo, K.H., Shek, C.H. and Lai, J.K.L. (2009). Recent developments in stainless steels. *Mater. Sci. Eng.: R: Reports*, **65(4)**: 39-104.

McGuire, M.F. (2008) Austenitic stainless steels (Chapter 6) in: Stainless steels for design engineers, pp 69-78. ASM International.

Osoba, L.O. Gao, Z. and Ojo, O.A. (2013), Physical and numerical simulations study of heat input dependence of HAZ cracking in Nickel base superalloy IN 718. *J. Metall. Eng*., **2 (3)**:88-93.

Poorhaydari, K., Patchett, B.M. and Ivey, D.G. (2005). Estimation of cooling rate in the welding of plates with intermediate thickness. *Weld. J.*, **84(10)**: 149s-155s.

Speidel, M.O. (2006). Nitrogen containing austenitic stainless steels. *Materialwissenschaft und Werkstofftechnik*, **37(10)**:875-880.

Sudhakaran, R., Sivasakthivel, P.S., Nagaraja, S. and Eazhil, K.M. (2014). The effect of welding process parameters on pitting corrosion and microstructure of chromium-manganese stainless steel gas tungsten arc welded plates. *Procedia Eng*., **97**:790-799.

Urade, V.P. and Ambade, S.P. (2016). An overview of welded low nickel chrome-manganese austenitic and ferritic stainless steel. *J. Mater. Sci. Eng*., **5(231)**:2169-0022.

Van Warmelo, M.N. (2006). Susceptibility of 12% Cr steels to sensitization during welding of thick plates. M.Sc. The Thesis, University of Wollongong. 120p.

Vander Voort, G.F. (1999). Metallography: Principles and Practice, ASM International, Ohio.

World Stainless Steel Organisation (2016), Stainless steel and its family. http://www.stainless-steel-world.net/basicfacts/stainless-steel-and-its-families.html,